

Fast Biped Walking via A Reflexive Neuromuscular-like Controller

Tao Geng, Bernd Porr and Florentin Wörgötter

Abstract—In this paper, we present our design and experiments of a planar dynamic biped robot under control of a neuromuscular-like reflexive controller. Our reflexive controller is built with biologically inspired model neurons, which directly drive a muscle model implemented on the joint motors, allowing our biped robot to exploit its own natural dynamics and muscle properties to generate fast and somewhat robust walking gaits. In our experiments, the robot can reach a relative walking speed of 3.5 leg-lengths per second, which is faster than that of any other biped walking robot, and is also comparable to the fastest relative speed of human walking.

I. INTRODUCTION

Although many biped robots have been developed using various technologies, they are still well outperformed by their natural counterpart, humans, in some important aspects such as speed and robustness. While biped robots usually depend on position control or trajectory tracking control at least in some stages of their walking gaits, humans and animals use a totally different "technology", neuromuscular control, by which stable walking gaits emerge from the global entrainment between the neuro-musculo-skeletal system and the environment [1]. Moreover, in human and animal locomotion, the muscle plays more roles than an activator or a motor does in a walking robot. The intrinsic properties of active muscle tissue may be sufficient to produce smooth motions even in the absence of specifically programmed neural inputs [2]. The force-length-velocity property of muscles make them rapidly respond to any disturbances [3], facilitating stability during walking. These performances of muscles have tremendously simplified the control demands of the nervous system for walking.

In this paper, we present our design and experiments of a planar biped robot and its reflexive neuromuscular control network composed of biologically plausible model neurones and a simple muscle model that is simulated with a control algorithm implemented on DC geared motors. In the experiments, our biped robot attained a relative speed that is faster than any other biped robot, and is comparable even with that of humans.

This paper is organized as follows. First we describe the mechanical design of our biped robot named "RunBot". Next, we present the neural model of our reflexive networks and

the implementation of a simple muscle model. Then we demonstrate the result of biped walking experiments.

II. THE ROBOT

RunBot is 23 cm high, foot to hip joint axis. It has four joints: left hip, right hip, left knee, right knee. Each joint is driven by a modified RC servo motor. A hard mechanical stop is installed on the knee joints, preventing it from going into hyperextension, similar to the function of knee caps in animals. The built-in Pulse Width Modulation control circuits of the RC motors are disconnected while its built-in potentiometer is used to measure the joint angles. Each foot is equipped with a modified Piezo transducer to sense ground contact events. We constrain the robot only in the sagittal plane by a boom of one meter length. The robot is attached to the boom via a freely-rotating joint while the boom is attached to the central column with a universal joint (see Fig 1A). This boom structure has negligible influence on the dynamics of the robot in the sagittal plane, allowing it freely trip or fall.

Our design of RunBot has characteristics, e.g., small curved feet and forwardly located mass center, which facilitate its fast-speed walking and the exploitation of natural dynamics.

RunBot is equipped with small curved feet for following considerations:

- (a) Flat and big feet can pose great difficulty in fast walking, which can be seen clearly when humans try to walk with skis or swimming fins.
- (b) Passive biped robots are usually equipped with circular feet, which increases the basin of attraction of stable walking gaits, and makes the motion of the stance leg look smoother.
- (c) The rotation of the stance foot at the heel or the toe can amount to up to eighty percent of a normal human walking gait [4]. The curved feet of RunBot can also allow this kind of rolling movement naturally.

In our previous simulation study using a dynamics model of RunBot [5], we have found that the location of the center of the mass of RunBot's trunk have very evident influence on the stability and speed of the gaits. If the mass center of the trunk is located appropriately forward, stable range and walking speed can both be improved. Therefore, we assembled RunBot's trunk in such a way that its center of mass is located about 3 cm forward the axes of the hip joints.

III. THE NEURAL STRUCTURE OF OUR REFLEXIVE CONTROLLER

A reflex is a local motor response to local sensation. In locomotion of human and animals, there exists evidence that

Manuscript received xxxxxx, 2005.

Tao Geng is with Department of Psychology, University of Stirling, Stirling FK9 4LA, UK

Bernd Porr is with Department of Electronics & Electrical Engineering, University of Glasgow, Glasgow, GT12 8LT, UK

Florentin Wörgötter is with Bernstein Centre for Computational Neuroscience, University of Göttingen, MPI für Dynamik und Selbstorganisation, Bunsenstr 10, D - 37073, Göttingen, Germany

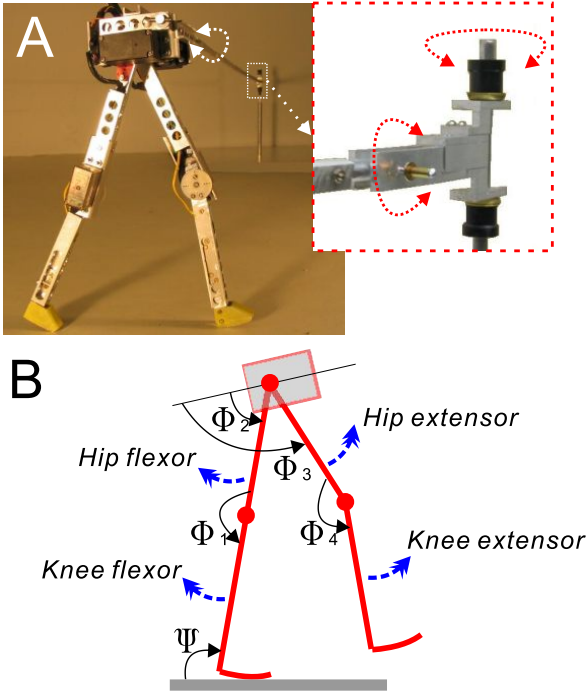


Fig. 1. (A). The robot, RunBot, and its boom structure. The three orthogonal axis of the boom indicated with curved arrows rotate freely. (B). Dynamics model of RunBot and the definitions of its joint angles.

various reflexes act together in an integrative manner to control and finally regulate the locomotive cycle [6]. Cruse developed a completely decentralized reflexive controller model to understand the locomotion control of walking in stick insects (*Carausius morosus*, [7]), which can immensely decrease the computational burden of the locomotion controller. With this eminent advantage, Cruse's reflexive controller and its variants have been implemented on some multi-legged robots [8]. Whereas in the case of biped robots, due to the unique problem of their intrinsic instability, reflexes usually work as an auxiliary function or as infrastructural units for other non-reflexive high-level or parallel controllers [9], [10]. To our knowledge, our RunBot is the first real-time dynamic biped exclusively controlled by a pure reflexive controller. Although the reflexive controller itself cannot directly control the walking stability, its coupling with the properly designed mechanics of RunBot has substantially ensured the stability of the dynamic biped gaits as will be shown in the experiments below.

The reflexive walking controller of RunBot is a simplified version of our former design [11]. It follows a hierarchical structure (see Fig 2). The bottom level is the reflex circuit local to the joints, including motor-neurons and angle sensor neurons involved in the joint reflexes. The top level is a distributed neural network consisting of hip stretch receptors and ground contact sensor neurons, which modulate the local reflexes of the bottom level. Neurons are modelled as non-spiking neurons simulated on a Linux PC, and communicated to the robot via the DA/AD board. Though somewhat simplified, they still

retain some of the prominent neuronal characteristics.

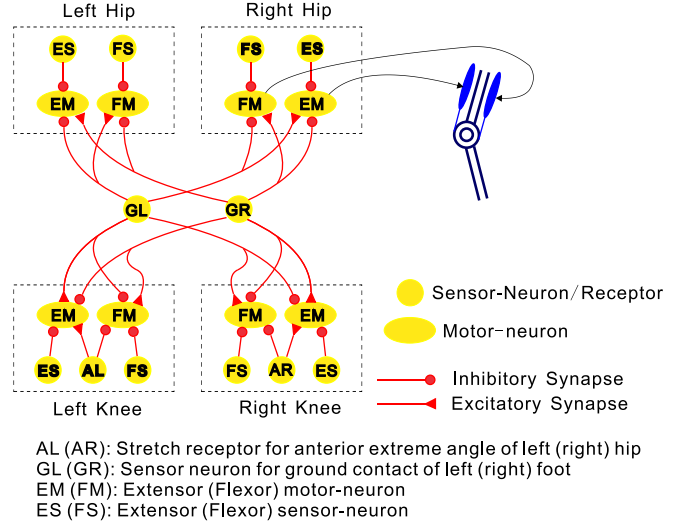


Fig. 2. The neuron model of reflexive controller on RunBot. Only the muscle pair of one joint is illustrated. Other joints are omitted.

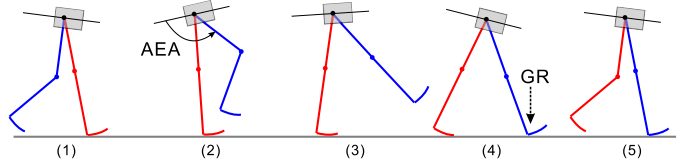


Fig. 3. Series of frames of one walking step. At the time of frame (3), The stretch receptor (AEA signal) of the swing leg is activated, which triggers the extensor of the knee joint in this leg. At the time of frame (7), the swing leg begin to touch the ground. This ground contact signal triggers the hip extensor and knee flexor of the stance leg, as well as the the hip flexor and knee extensor of the swing leg. Thus the swing leg and the stance leg swap their roles thereafter.

A. Model neuron circuit of the top level

The joint coordination mechanism in the top level is implemented with the neuron circuit illustrated in Fig 2. Each of the ground contact sensor neurons has excitatory connections to the motor-neurons of the ipsi-lateral hip flexor and knee extensor as well as to the contra-lateral hip extensor and knee flexor. The stretch receptor of each hip has excitatory connections to its ipsi-lateral motor-neuron of the knee extensor, and inhibitory connection to its ipsi-lateral motor-neuron of the knee flexor. Detailed models of the stretch receptor, and ground contact sensor neuron are described in the following subsections.

1) *Stretch receptors*: Stretch receptors play a crucial role in animal locomotion control. When the limb of an animal reaches an extreme position, its stretch receptor sends a signal to the controller, resetting the phase of the limbs. While other biologically inspired locomotive models and robots use two stretch receptors on each leg to signal the attaining of the leg's AEP (Anterior Extreme Position) and PEP (Posterior Extreme Position) respectively, our robot has only one stretch receptor

on each leg to signal the AEA of its hip joint. Furthermore, the function of the stretch receptor on our robot is only to trigger the extensor reflex on the knee joint of the same leg, rather than to implicitly reset the phase relations between different legs as in the case of Cruse's model.

As the hip joint approaches the AEA, the output of the stretch receptors for the left (AL) and the right hip (AR) is increased as:

$$\rho_{AL} = \left(1 + e^{\alpha_{AL}(\Theta_{AL}-\phi)}\right)^{-1} \quad (1)$$

$$\rho_{AR} = \left(1 + e^{\alpha_{AR}(\Theta_{AR}-\phi)}\right)^{-1} \quad (2)$$

Where ϕ (representing ϕ_2 or ϕ_3 , see Fig 1B) is the real time angular position of the hip joint, Θ_{AL} and Θ_{AR} are the hip anterior extreme angles, α_{AL} and α_{AR} are positive constants. This model is inspired by a sensor neuron model presented in [12] that is thought capable of emulating the response characteristics of populations of sensor neurons in animals.

The definition and direction of the joint angles is illustrated in Fig 1B. The direction of extensor on both hip and knee joints is forward while that of flexors is backward.

2) *Ground contact sensor neurons*: Another kind of sensor neuron incorporated in the top level is the ground contact sensor neuron, which is active when the foot is in contact with the ground. Its output, similar to that of the stretch receptors, changes according to:

$$\rho_{GL} = \left(1 + e^{\alpha_{GL}(\Theta_{GL}-V_L+V_R)}\right)^{-1} \quad (3)$$

$$\rho_{GR} = \left(1 + e^{\alpha_{GR}(\Theta_{GR}-V_R+V_L)}\right)^{-1} \quad (4)$$

Where V_L and V_R are the output voltage signals from piezo sensors of the left foot and right foot respectively, Θ_{GL} and Θ_{GR} work as thresholds, α_{GL} and α_{GR} are positive constants.

While AEP and PEP signals account for switching between stance phase and swing phase in other walking control structures, ground contact signals play a crucial role in phase transition control of our reflexive controller. In PEP/AEP-models, the movement pattern of a leg will break down as soon as the AEP or PEP can not be reached, which may happen as a consequence of an unexpected disturbance from the environment or due to intrinsic failure. This can be catastrophic for a biped, though tolerable for a hexapod due to its high degree of redundancy.

B. Neural circuit of the bottom level

In animals, a reflex is triggered in response to a suprathreshold stimulus. The quickest reflex in animals is the "monosynaptic reflex", in which the sensor neuron directly contacts the motor-neuron. The bottom-level reflex system of our robot consists of reflexes local to each joint (see Fig 2). The neuron module for one reflex is composed of one angle sensor neuron and the motor-neuron it contacts (see Fig 2). Each joint is equipped with two reflexes, extensor reflex and flexor reflex, both are modelled as a monosynaptic reflex, that is, whenever its threshold is exceeded, the angle sensor neuron directly excites the corresponding motor-neuron. In addition, the motor-neurons of the local reflexes also receive an excitatory synapse

and an inhibitory synapse from the neurons of the top level, by which the top level can modulate the bottom-level reflexes.

Each joint has two angle sensor neurons, one for the extensor reflex, and the other for the flexor reflex (see Fig 2). Their models are similar to that of the stretch receptors described above. The extensor angle sensor neuron changes its output according to:

$$\rho_{ES} = \left(1 + e^{\alpha_{ES}(\Theta_{ES}-\phi)}\right)^{-1} \quad (5)$$

where ϕ is the real time angular position obtained from the potentiometer of the joint (see Fig 1B). Θ_{ES} is the threshold of the extensor reflex and α_{ES} a positive constant.

Likewise, the output of the flexor sensor neuron is modelled as:

$$\rho_{FS} = \left(1 + e^{\alpha_{FS}(\phi-\Theta_{FS})}\right)^{-1} \quad (6)$$

with Θ_{FS} and α_{FS} similar as above.

In order to make the movements of the thighs symmetric around the trunk like human's walking gaits, we add this constraint,

$$\Theta_{ES,h} + \Theta_{FS,h} = 180deg \quad (7)$$

Where $\Theta_{ES,h}(\Theta_{FS,h})$ is the threshold of the extensor (flexor) sensor-neurons of the hip joints.

The equations of the extensor/flexor sensor-neurons seem the same as those of the AEA stretch receptors. But, in fact, their effects are fundamentally different. The extensor/flexor sensor-neurons work locally, that is, it only belongs to the local reflex module of the single joint, and only affect the movement of the local joint, being not visible to control modules of any other joints or legs. Whereas the phasic feedback signals like AEP (or AEA in RunBot) work at inter-joint level. One important property of distributed control systems like the reflexive controller is that most of the local sensor signals or local information are processed locally and only have local influences, which makes the system more robust.

The motor-neuron model is adapted from one used in the neural controller of a hexapod simulating insect locomotion [13]. The state and output of each extensor motor-neuron is governed by following equations [14] (those of flexor motor-neurons are similar):

$$\lambda \frac{dy}{dt} = -y + \sum \omega_X \rho_X \quad (8)$$

$$M_E = \left(1 + e^{\Theta_{EM}-y}\right)^{-1} \quad (9)$$

Where y represents the mean membrane potential of the neuron. Equation 9 is a sigmoidal function that can be interpreted as the neuron's short-term average firing frequency, Θ_{EM} is a bias constant that controls the firing threshold. λ is a time constant associated with the passive properties of the cell membrane [14], ω_X represents the connection strength from the sensor neurons and stretch receptors to the motor-neuron (Fig 2). ρ_X represents the output of the sensor-neurons and stretch receptors that contact this motor-neuron (e.g., ρ_{ES} , ρ_{AL} , ρ_{GL} , etc.) M_E and M_F are the outputs of the extensor- and flexor motor-neurons, respectively, which directly drive the muscle model that will be described below.

The model neuron parameters are listed in . The time constants λ of motor-neurons take the same value of 3ms.

The weights of all the inhibitory connections are set to -10, except those between sensor-neurons and motor-neurons, which are -30, and those between stretch receptors and flexor motor-neurons, which are -15. The weights of all excitatory connections are 10, except those between stretch receptors and extensor motor-neurons, which are 15.

Our reflexive network has some evident differences from Cruse's model. Cruse's model depends on PEP, AEP and GC (Ground Contact) signals to generate the movement pattern of the individual legs. Whereas our reflexive controller presented here uses only GC and AEA signals to coordinate the movements of the joints. Moreover, the AEA signal of each hip in RunBot only acts on the knee joint belonging to the same leg, not functioning on the leg-level as the AEP and PEP did in Cruse's model. The use of fewer phasic feedback signals has further simplified the controller structure in RunBot.

IV. IMPLEMENTING A MUSCLE MODEL IN THE ROBOT

We use a linear viscous elastic muscle model that is composed of a spring in parallel with a viscous damper, and is directly controlled by the motor-neuron output [12]. Each joint has an antagonistic muscle pair of flexor and extensor, which are activated by extensor- and flexor motor-neuron, respectively (see Fig 2). The torque exerted by the muscle pair on one joint (for example, the joint indicated with ϕ_1 in Fig 1B), T_1 , can be described as [12],

$$T_1 = K(\phi_1 - L) - \delta\dot{\phi}_1 \quad (10)$$

$$K = \beta(M_E + M_F + \gamma) \quad (11)$$

$$L = \alpha(M_E - M_F)/K + L_0 \quad (12)$$

Where K is the effective stiffness of the muscle pair, L the resting angle of the muscle pair, and L_0 an offset. α and β are gains. γ is a base level of stiffness, δ the damping coefficient. For details of this muscle model, see [12].

Before we can implement this muscle model in RunBot, we have to do some analysis on the dynamics of the robot and its joint motors.

The dynamics of RunBot are modelled as shown in Fig 1B. With the Lagrange method, we can get the equations that govern the motion of the robot, which can be written in the form:

$$D(q)\ddot{q} + C(q, \dot{q}) + G(q) = \tau \quad (13)$$

Where $q = [\phi_1, \phi_2, \phi_3, \phi_4, \psi]^T$ is a vector describing the configuration of the robot (for definition of $\psi, \phi_1, \phi_2, \phi_3, \phi_4$, see Fig 1B). $D(q)$ is the 5×5 inertia matrix, $C(q, \dot{q})$ is the 5×1 vector of centripetal and coriolis forces, $G(q)$ is the 5×1 vector representing gravity forces. $\tau = [\tau_1, \tau_2, \tau_3, \tau_4, 0]^T$, $\tau_1, \tau_2, \tau_3, \tau_4$ are the torques applied on the joints.

The dynamics of the DC motor (including gears) of each joint can be described with the following equations (here, once again, the joint indicated with ϕ_1 in Fig 1B is taken as an example. The models of other joints are likewise):

$$L_a \frac{di_a}{dt} + R_a i_a + nk_3 \dot{\phi}_1 = V_1 \quad (14)$$

$$\tau_1 + I_1 \ddot{\phi}_1 + k_f \dot{\phi}_1 = nk_2 i_a \quad (15)$$

Where, V_1 is the applied armature voltage of the motor, i_a is the armature current, L_a the armature inductance, R_a the armature resistance. k_3 is the emf constant. k_2 is the motor torque constant. I_1 is the combined moment of inertial of the joint motor and gear train referred to the gear output shaft. k_f is the viscous-friction coefficient of the combination of the motor and the gear. n is the gear ratio.

Considering that the electrical time-constant of the motor is much smaller than the mechanical time-constant of the robot, we neglect the dynamics of the electrical circuits of the motor, which leads to, $\frac{di_a}{dt} = 0$. Thus equation 14 is reduced to,

$$i_a = \frac{1}{R_a} (V_1 - nk_3 \dot{\phi}_1) \quad (16)$$

Let

$$\hat{\tau} = \tau + I\ddot{q} \quad (17)$$

$$\text{Where } \hat{\tau} = \begin{pmatrix} \hat{\tau}_1 \\ \hat{\tau}_2 \\ \hat{\tau}_3 \\ \hat{\tau}_4 \\ 0 \end{pmatrix}, I = \begin{pmatrix} I_1 & 0 & 0 & 0 & 0 \\ 0 & I_2 & 0 & 0 & 0 \\ 0 & 0 & I_3 & 0 & 0 \\ 0 & 0 & 0 & I_4 & 0 \\ 0 & 0 & 0 & 0 & 0 \end{pmatrix}$$

I_i is the combined moment of inertial of the joint motors and gear trains referred to the gear output shaft.

Combining equations 13 and 17, we can describe the dynamics of the robot in a new form with $\hat{\tau}$ as the torque input.

$$(D(q) + I)\ddot{q} + C(q, \dot{q}) + G(q) = \hat{\tau} \quad (18)$$

Combining equations 15, 16, and 17, we can get

$$\hat{\tau}_1 = \frac{nk_2}{R_a} V_1 - \left(\frac{n^2 k_2 k_3}{R_a} + k_f \right) \dot{\phi}_1 \quad (19)$$

We apply following control algorithm on the input voltage of this joint motor,

$$V_1 = \frac{R_a K}{nk_2} (\phi_1 - L) - \left(\frac{R_a (\delta - k_f)}{nk_2} - nk_3 \right) \dot{\phi}_1 \quad (20)$$

Combining equations 19 and 20, we can get,

$$\hat{\tau}_1 = K(\phi_1 - L) - \delta\dot{\phi}_1 \quad (21)$$

Now from the equations 10, 11, 12, 18, and 21, we can see that the muscle model has been implemented on this joint. Likewise, we can obtain the control algorithm for applying the muscle model on other joints.

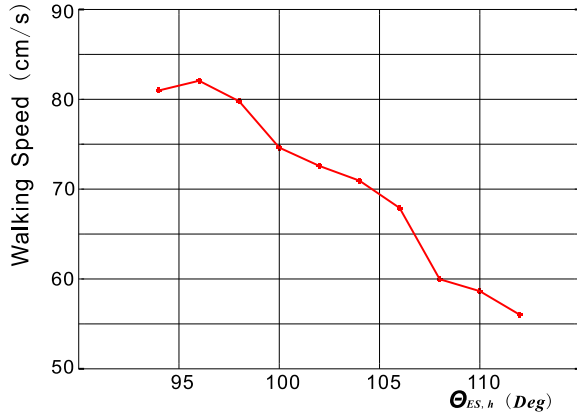


Fig. 4. The change of walking speed while $\Theta_{ES,h}$ is tuned manually. If $\Theta_{ES,h} < 94$ Deg, the robot tends to fall forward in a few steps. If $\Theta_{ES,h} > 112$ Deg, the robot ends to fall backward in a few steps.

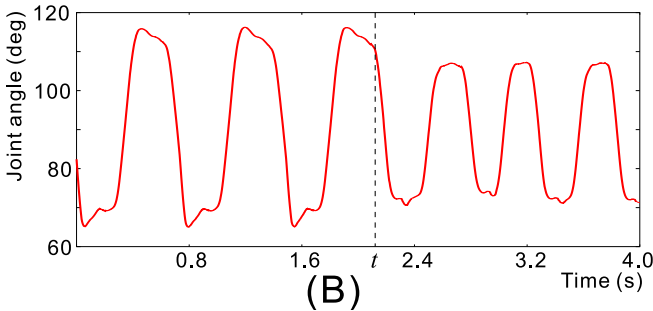
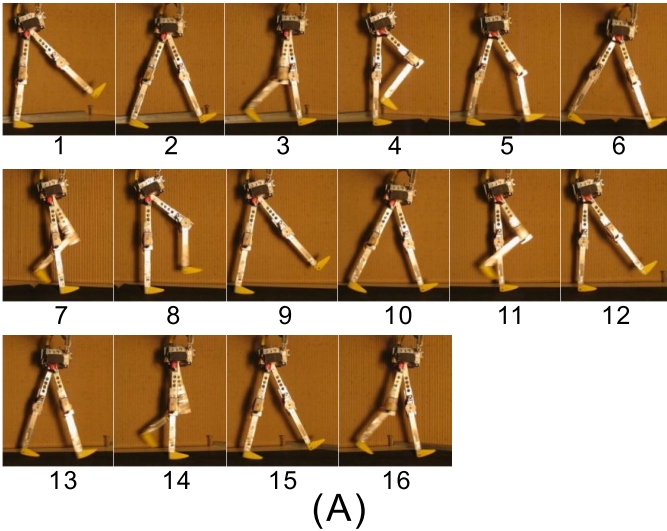


Fig. 5. (A) Series of sequential frames of the walking gait. $\Theta_{ES,h}$ is changed from 110 deg to 95 deg at the time of frame (10). The interval between two adjacent frames is 100 ms. (B) Real-time data of the angular position of one hip joint while the $\Theta_{ES,h}$ is changed at time t . To eliminate the noises in the potentiometer signals, we use a first-order filter.

V. ROBOT WALKING EXPERIMENTS

In biped robots, it is a puzzling problem how to change its walking speed on the fly without undermining its dynamical stability at the same time. RunBot's walking speed can be changed on the fly by tuning $\Theta_{ES,h}$ (of course, $\Theta_{FS,h}$ is

also changed accordingly with equation 7). Fig 4 shows the relationship between the walking speed and $\Theta_{ES,h}$.

Figure 5A shows the gait when $\Theta_{ES,h}$ is changed greatly and abruptly from 110 deg to 95 deg at a time t (indicated with a line in figure 5B). The walking speed is immediately changed from 57 cm/s to a fast one (82 cm/s). Although there is no specifically designed controller in charge of the sensing and control of the transient stage of speed-changing, the natural dynamics of the robot itself and the muscle model properties ensure stability during the change. The video clip of this experiment can be seen at, <http://www.cn.stir.ac.uk/~tgeng/smc/speedchange.mpg>

To compare the walking speed of various biped robots whose sizes are quite different from each other, we use the relative speed, speed divided by the leg-length. We know of no other biped robot attaining such a fast relative speed as RunBot's (see figure /refotherrobotsfig. Moreover, RunBot's highest relative walking speed is comparable to that of humans. To get a feeling of how fast RunBot can walk, we strongly encourage readers to watch the video clip.


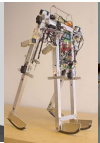
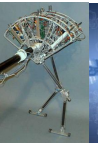



						
Leg length (m)	0.8	0.75	0.9	0.8	0.23	3.94
Max. speed (m/s)	0.6	0.40	1.25	1.20	0.82	
Relative Speed	0.7	0.5	1.4	1.5	3.5	4~5
	(a)	(b)	(c)	(d)	(e)	(f)

Fig. 6. Relative leg-length and Maximum relative speed of various planar biped robots. (a) A copy of McGeer's planar passive biped robot walking down a slope [15]. (b) "Mike", similar to McGeer's robot, but equipped with pneumatic actuators at its hip joints. Thus it can walk half-passively on level ground [15]. (c) "Spring Flamingo", a powered planar biped robot with actuated ankle joints [16]. (d) Rabbit, a powered biped with 4 degree-of-freedom and point feet. (e) RunBot. (f) Olympic record of human's walking speed.

As shown in figure 7, with a small value of $\Theta_{ES,h}$ (95 deg), RunBot can walk up a shallow slope. Figure 7 shows a series frames of RunBot's gait walking up a shallow slope of 0.05 rad (but any bigger slope cannot be overcome). Note, RunBot can neither detect the slope nor adjust any parameters of its controller to address it. For the video footage of this experiment, see <http://www.cn.stir.ac.uk/~tgeng/smc/slope.mpg>

VI. CONCLUSION

Using real-time experiments, this study has shown that fast dynamic biped walking can be achieved via neuromuscular-like reflexive controller without needing any trajectory control mechanisms. The natural dynamics of the robot and the viscous elastic muscle model implemented on its joints have contributed substantially to the motion generation and robustness of the walking gaits, thus simplifying the controller structure.

REFERENCES

- [1] Gentaro Taga. A model of the neuro-musculo-skeletal systems for human locomotion. *Biological Cybernetics*, 73:97–111, 1995.

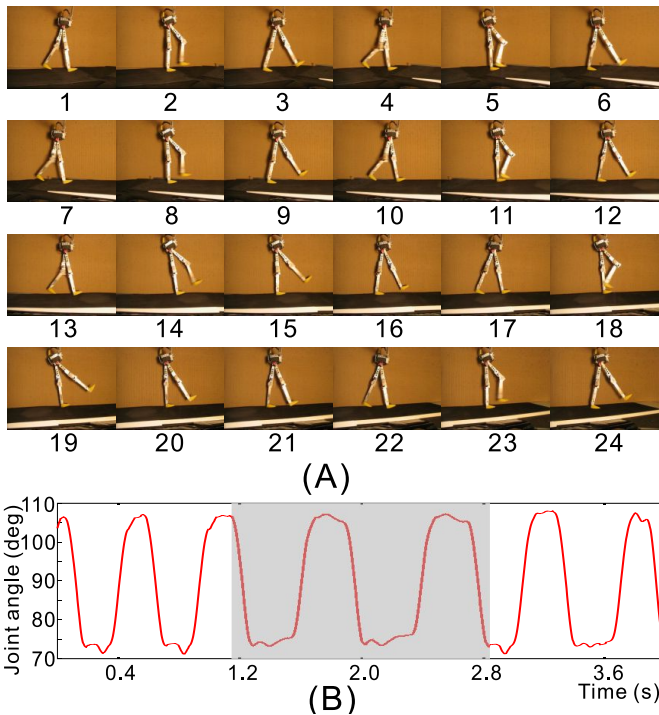


Fig. 7. (A). Runbot is walking up a shallow slope of 0.05 rad. The time interval is 100 ms. Frames (1)-(9) are the normal gait on the flat floor. Frames (10)-(16) are the gaits on the slope. The frames after (16) shows that the gaits return to normal on a flat surface. (B). Real-time data of the angular position of one hip joint while Runbot is walking up the slope (the shaded area).

2d autonomous biped based on passive dynamic walking. In *Proceedings of 2nd International Symposium on Adaptive Motion of Animals and Machines*, Kyoto, Japan, 2003.

- [16] J. Pratt. *Exploiting Inherent Robustness and Natural Dynamics in the Control of Bipedal Walking Robots*. PhD thesis, Massachusetts Institute of Technology, 2000.

- [2] M. Andrew and W. Rymer. Role of intrinsic muscle properties in producing smooth movements. *IEEE Transactions on Biomedical Engineering*, 44:165–176, 1997.
- [3] KGM Gerritsen. Intrinsic muscle properties facilitate locomotor control - a computer simulation study. *Motor Control*, 2:206–220, 1998.
- [4] Michael Hardt and Oskar von Stryk. The role of motion dynamics in the design, control and stability of bipedal and quadrupedal robots. In *RoboCup*, pages 206–223, 2002.
- [5] T. Geng, B. Porr, and F. Wörgötter. Fast biped walking with a sensor-driven neuronal controller and real-time online learning. *International Journal of Robotics Research (submitted)*, 2005.
- [6] E. Paul Zehr and Richard B. Stein. What functions do reflexes serve during human locomotion? *Progress in Neurobiology*, 58:15–205, 1999.
- [7] H. Cruse, T. Kindermann, M. Schumm, and et.al. Walknet - a biologically inspired network to control six-legged walking. *Neural Networks*, 11(7-8):1435–1447, 1998.
- [8] C. Ferrell. A comparison of three insect-inspired locomotion controllers. *Robotics and Autonomous Systems*, 16:135–159, 1995.
- [9] G. Boone and J. Hodgins. Slipping and tripping reflexes for bipedal robots. *Autonomous Robots*, 4(3):259–271, 1997.
- [10] H. Funabashi, Y. Takeda, Itoh. S., and M. Higuchi. Disturbance compensating control of a biped walking machine based on reflex motions. *JSME International Journal Series C-Mechanical Systems, Machine Elements and Manufacturing*, 44:724–730, 2001.
- [11] T. Geng, B. Porr, and F. Wörgötter. Coupling of neural computation with physical computation for stable dynamic biped walking control. *Neural Computation (in press)*, 2005.
- [12] T. Wadden and O. Ekeberg. A neuro-mechanical model of legged locomotion: Single leg control. *Biological Cybernetics*, 79:161–173, 1998.
- [13] R.D. Beer and H.J. Chiel. A distributed neural network for hexapod robot locomotion. *Neural Computation*, 4:356–365, 1992.
- [14] J.C. Gallagher, R.D. Beer, K.S. Espenschied, and R.D. Quinn. Application of evolved locomotion controllers to a hexapod robot. *Robotics and Autonomous Systems*, 19:95–103, 1996.
- [15] M. Wisse and J. van Frankenhuyzen. Design and construction of mike; a